

1

2 *In Vivo* Activation of Human NK cells by Treatment with an IL-15 Superagonist Potently  
3 Inhibits Acute *In Vivo* HIV-1 Infection in Humanized Mice

4

5 Kieran Seay<sup>a</sup>, Candice Church<sup>a</sup>, Jian Hua Zheng<sup>b</sup>, Kathryn Deneroff<sup>b</sup>, Christina  
6 Ochsenbauer<sup>c</sup>, John C. Kappes<sup>c,d</sup>, Bai Liu<sup>e</sup>, Emily K. Jeng<sup>e</sup>, Hing C. Wong<sup>e</sup>  
7 and Harris Goldstein<sup>a,b,#</sup>

8

9 **Author affiliation:**

10 Departments of <sup>a</sup>Microbiology & Immunology and <sup>b</sup>Pediatrics, Albert Einstein College of  
11 Medicine, Bronx, New York, USA.

12 <sup>c</sup>Department of Medicine, University of Alabama at Birmingham, <sup>d</sup>Birmingham Veterans  
13 Affairs Medical Center, Research Service, Birmingham, Alabama, USA

14 <sup>e</sup>Altor BioScience Corporation, Miramar, Florida, USA

15

16 **Running Head:** NK Cell Activation Inhibits *In Vivo* HIV Infection

17

18 **#Address correspondence to:** Harris Goldstein, harris.goldstein@einstein.yu.edu

19

20 KS and CC contributed equally to this work

21

22 **Word Count:** Abstract- 250 words Text- 5,239 words

23

24 **Abstract**

25 Natural killer (NK) cells with anti-HIV-1 activity may inhibit HIV-1 replication and  
26 dissemination during acute HIV-1 infection. We hypothesized that the NK cell capacity  
27 to suppress acute *in vivo* HIV-1 infection would be augmented by activating them via  
28 treatment with an IL-15 superagonist, IL-15 bound to soluble IL-15R $\alpha$ , an approach that  
29 potentiates human NK cell-mediated killing of tumor cells. *In vitro* stimulation of human  
30 NK cells with a recombinant IL-15 superagonist significantly induced their expression of  
31 cytotoxic effector molecules granzyme B and perforin, their degranulation upon  
32 exposure to K562 cells as indicated by cell-surface expression of CD107a and their  
33 capacity to lyse K562 cells and HIV-1-infected T cells. The impact of IL-15  
34 superagonist-induced activation of human NK cells on acute *in vivo* HIV-1 infection was  
35 investigated using hu-spl-PBMC-NSG mice, NOD-SCID-IL2 $\gamma$ <sup>-/-</sup> mice intrasplenically  
36 injected with human PBMCs, which develop productive *in vivo* infection after  
37 intrasplenic inoculation with HIV-1. IL-15 superagonist treatment potently inhibited acute  
38 HIV-1 infection in hu-spl-PBMC-NSG mice even when delayed until three days after  
39 intrasplenic HIV-1 inoculation. Removal of NK cells from the human PBMCs prior to  
40 intrasplenic injection into NSG mice completely abrogated IL-15 superagonist-mediated  
41 suppression of *in vivo* HIV-1 infection. Thus, the *in vivo* activation of NK cells, integral  
42 mediators of the innate immune response, by treatment with an IL-15 superagonist  
43 increases their anti-HIV activity and enables them to potently suppress acute *in vivo*  
44 HIV-1 infection. These results indicate that *in vivo* activation of NK cells may represent a  
45 new immunotherapeutic approach to suppress acute HIV-1 infection.

46

47 **Importance**

48           Epidemiological studies have indicated that NK cells contribute to the control of  
49 HIV-1-infection and *in vitro* studies have demonstrated that NK cells can selectively kill  
50 HIV-1-infected cells. We demonstrated that *in vivo* activation of NK cells by treatment  
51 with an IL-15 superagonist that potently stimulates the anti-tumor activity of NK cells  
52 markedly inhibited acute HIV-1 infection in humanized mice, even when activation of the  
53 NK cells by IL-15 superagonist treatment is delayed until 3 days after HIV-1 inoculation.  
54 NK cell-depletion from the PBMCs prior to their intrasplenic injection abrogated the  
55 suppression of *in vivo* HIV-1-infection observed in humanized mice treated with the IL-  
56 15 superagonist, demonstrating that the activated human NK cells were mediating IL-15  
57 superagonist-induced inhibition of acute HIV-1 infection. Thus, *in vivo*  
58 immunostimulation of NK cells, a promising therapeutic approach for cancer therapy,  
59 may represent a new treatment modality for HIV-1-infected individuals particularly in the  
60 earliest stages of infection.

61

62

63

64

65

66 **Introduction**

67           The crucial role of the HIV-specific T cell and antibody response mounted by the  
68 adaptive immune system to control HIV-1 infection is well established (1). However,  
69 during acute infection viremia is not controlled because it takes several weeks after the  
70 initiation of infection for the adaptive immune response to activate and clonally expand  
71 sufficient HIV-1-specific T cells and B cells to suppress HIV-1 infection (2). This delay in  
72 the mobilization of the adaptive immune response permits HIV-1 to rapidly replicate and  
73 disseminate during the acute phase of infection leading to the production of high plasma  
74 viral loads which are associated with an adverse disease course (3, 4). Early control of  
75 HIV-1 replication can have a beneficial impact on subsequent disease course as  
76 evidenced by the ability of some individuals whose viremia was suppressed by  
77 combination antiretroviral therapy (cART) during acute infection to achieve long-term  
78 infection control despite lacking protective HLA B alleles (5-7). Prior to the development  
79 of an effective HIV-1-specific adaptive immune response, NK cells, crucial innate  
80 immune effector cells which are large granular cytotoxic lymphocytes, are rapidly  
81 activated and expanded and may contribute to controlling the initial phase of HIV-1  
82 replication (8, 9). Infection induces changes in the cellular expression of ligands  
83 recognized by NK cell receptors which enables NK cells to specifically identify and kill  
84 virally infected cells to control and/or abort viral infections prior to the initiation of  
85 antigen-specific responses (10). One mechanism by which HIV-1-infected cells become  
86 susceptible to killing by NK cells is through the reduction in their surface expression of  
87 MHC Class I molecule expression mediated by HIV-1 Nef as a means of evading killing  
88 by HIV-1-specific CD8+ cytotoxic T cells (11). Further support for the role of NK cells in

89 controlling HIV-1 replication and improving clinical outcomes is provided by several  
90 genetic population studies linking slower HIV-1 disease progression with the expression  
91 of specific allotypes of killer cell immunoglobulin-like receptors (KIRs) and their  
92 respective HLA-class I ligands (10). However, the correlates of protective HIV-1-specific  
93 immunity conferred by NK cells are not well characterized and there is no direct  
94 evidence that *in vivo* stimulation of NK cell activity can enhance their capacity to inhibit  
95 acute *in vivo* HIV-1 infection.

96       After infection, NK cells are rapidly activated by IL-15, a multifunctional cytokine  
97 produced by activated dendritic cells and macrophages, which enables NK cells to  
98 generate protective responses capable of clearing viral infections (12-14). In contrast to  
99 IL-2 and other cytokines which are secreted and circulate until they bind directly to their  
100 cognate receptors on target cells, IL-15 secreted by dendritic cells and macrophages  
101 binds to the IL-15-specific receptor alpha chain (IL-15R $\alpha$ /CD215) embedded on their  
102 cell-surfaces to form a membrane-bound IL-15:IL-15R $\alpha$  complex. This complex is then  
103 presented in *trans* to bind to the IL-15R $\beta$  (IL-2R $\beta$ /CD122) and IL-15R $\gamma$  (IL-2R $\gamma$ /CD132)  
104 chains expressed by adjacent NK cells and CD8<sup>+</sup> T cells which activate them (13, 15).  
105 Alternatively, IL-15:IL-15R $\alpha$  complexes are cleaved from dendritic cell and macrophage  
106 membranes and are released into the serum, where they circulate as stable  
107 heterodimers which display greater *in vivo* bioactivity and half-life (4 hours vs. 30  
108 minutes) than secreted IL-15 monomers (16) to potently stimulate NK cells and/or CD8<sup>+</sup>  
109 T cells to eliminate virally infected cells (17). Consequently, the functional activity of  
110 recombinant IL-15 can be greatly augmented by complexing it with soluble recombinant  
111 IL-15R $\alpha$  and thereby converting IL-15 from an agonist to a superagonist (6). To replicate

112 the increased functional activity of the IL-15:IL-15R $\alpha$  complex, we constructed a fusion  
113 protein, IL-15N72D:IL-15R $\alpha$ Su/Fc (IL-15 superagonist), which consists of two linked  
114 IgG1 Fc domains, each fused to an IL-15R  $\alpha$ -chain 65-aa binding region spanning the  
115 Sushi (Su) domain (18). The Sushi domain is then bound to IL-15N72D, an IL-15  
116 molecule with the aspartic acid at position 72 mutated to asparagine which increases its  
117 affinity for the human IL-15R $\beta$ -chain and its biological activity by ~5-fold as compared to  
118 native human IL-15 (19). As a consequence of these structural modifications, the IL-15  
119 superagonist, identified as ALT-803 for Phase I studies evaluating its efficacy as a  
120 candidate cancer therapeutic, exhibits ~25-fold higher biological activity and >35-fold  
121 longer serum half-life (~25 hours vs. ~40 minutes) than soluble IL-15 and potently  
122 stimulates *in vivo* NK cell and CD8<sup>+</sup> T cell proliferation in mice (20). In the current study,  
123 we investigated whether the capacity of NK cells to inhibit acute HIV-1 infection could  
124 be stimulated by the *in vivo* administration of the IL-15 superagonist to humanized mice  
125 days after inoculation with HIV-1. For these experiments we used a humanized mouse  
126 model, hu-spl-PBMC-NSG mice, generated by intrasplenically injecting NOD-SCID  
127 IL2r $\gamma$ <sup>-/-</sup> (NSG) mice with activated human peripheral blood mononuclear cells (PBMCs),  
128 which develop rapid and robust HIV-1 infection after intrasplenic inoculation with HIV-1.

129 **Materials and Methods**

130 *Generation of HIV-1 infectious molecular clones.* Virus stocks were generated by  
131 transient transfection of 293T cells with a plasmid, NL-LucR.T2A-JR-CSF.ecto, which  
132 encodes an infectious HIV-1 molecular clone whose Env protein ectodomain sequence  
133 is derived from the JR-CSF Env and which expresses the *Renilla reniformis* luciferase  
134 (LucR) gene (HIV-LucR) as previously described (21). LucR has a short cellular half-life  
135 of approximately 3 hours (22), so its expression reflects active replication. HIV-LucR,  
136 which was engineered to express the LucR reporter gene and the heterologous JR-CSF  
137 *env* gene in *cis* with all of the HIV-1 open reading frames, continues to express LucR  
138 over multiple cycles of replication after inoculation permitting highly sensitive and  
139 specific detection of active HIV-1 replication for several weeks after inoculation (21).  
140 The infectious titer of the HIV-LucR virus [5- to 10 x 10<sup>7</sup> infectious units (IU)/ml] was  
141 determined by limiting dilution infection of TZM-bl cells as described (21).

142 *Generation of the IL-15 superagonist fusion complex.* The expression vector  
143 pMSGV-IL-15R $\alpha$ Su/Fc expressing the IL-15R $\alpha$ Su/Fc fusion gene was constructed by  
144 overlap PCR amplification of DNA templates encoding the Su domain of human IL-15R $\alpha$   
145 (aa1–65 of human IL-15R $\alpha$ ) and the human IgG1 Fc fragment and was ligated into the  
146 pMSGV-1 expression vector as described (23). To bind to the two IL-15 binding sites in  
147 the IL-15R $\alpha$ Su/Fc fusion protein, we used IL-15N72D, human IL-15 mutated to replace  
148 the native aspartic acid at position 72 with an asparagine. This IL-15 mutein displays a  
149 ~5-fold higher levels of biological activity than the native IL-15 due to its increased  
150 affinity and binding to the human IL-15R $\beta$ -chain (19). The complex of IL-15R $\alpha$ Su/Fc  
151 bound to IL-15N72D (IL-15 superagonist) was generated by co-transfecting expression

152 vectors encoding IL-15R $\alpha$ Su/Fc and IL-15N72D into CHO cells and purifying the soluble  
153 the IL-15 superagonist fusion protein complex using a two-step affinity and ion  
154 exchange chromatography-based process as described (20).

155 *Measurement of the in vivo capacity of the IL-15 superagonist to inhibit in vivo*  
156 *HIV-1 infection.* NOD-SCID IL2 $\gamma$ <sup>-/-</sup> (NSG) mice (Jackson Laboratories, Bar Harbor, ME)  
157 were bred and maintained under isolation and biocontainment conditions as described  
158 (24). The *in vivo* anti-HIV-1 activity of the IL-15 superagonist was determined using  
159 humanized mice generated through a modification of an *in vivo* adoptive transfer system  
160 we developed (25). PBMCs isolated from HIV-1 naïve donors were cultured in RPMI  
161 1640 supplemented with 10% heat-inactivated fetal bovine serum, penicillin (100 U/ml),  
162 streptomycin (10  $\mu$ g/ml), glutamine (2 mM) and HEPES (10 mM) and activated with  
163 phytohemagglutinin (PHA) (4  $\mu$ g/ml) and IL-2 (100 U/ml) for 24 hours, washed and  
164 resuspended ( $\sim 8 \times 10^7$  cells/ml) in sterile cold PBS. NSG mice were intrasplenically  
165 injected with the activated human PBMCs ( $\sim 8 \times 10^6$  cells) to generate hu-spl-PBMC-  
166 NSG mice. Some of the hu-spl-PBMC-NSG mice were challenged *in vivo* with HIV-1 by  
167 intrasplenic injection with 100  $\mu$ L of HIV-LucR virus ( $1 \times 10^8$  IU/ml) in parallel with  
168 intrasplenic injection of the activated PBMCs. One or three days after intrasplenic HIV-1  
169 challenge, the mice were treated with one intravenous dose of the IL-15 superagonist  
170 (0.2 mg/kg) which provides the mice with a serum C<sub>max</sub> of  $\sim 25$  nM. For some  
171 experiments, the PBMCs were depleted of CD8<sup>+</sup> T cells or NK cells (>95% depletion)  
172 prior to their injection into the mice by immunomagnetic sorting using anti-human CD8  
173 or anti-human CD56 microbeads (Miltenyi Biotec, Cambridge, MA). The level of HIV-1  
174 infection that developed in the transferred human PBMCs in the spleens of the hu-spl-

175 PBMC-NSG mice was quantified by measuring the LucR activity in the mouse splenic  
176 lysates using the Renilla Luciferase Assay System (Promega, Madison, WI) as  
177 described (26). To visualize and quantify *in vivo* HIV-1 infection using bioluminescent  
178 imaging, mice were imaged with the IVIS Spectrum imager (Caliper LifeSciences,  
179 Hopkinton, MA) after intravenous injection (5 µg/mouse) of the bioluminescence  
180 substrate RediJect Coelenterazine h (Caliper Life Sciences) and the images were  
181 analyzed using the Wizard bioluminescent selection tool for automatic wavelength and  
182 exposure detection. The bioluminescent and gray-scale images were overlaid using the  
183 LivingImage 4.0 software package to create a pseudocolor image that represents  
184 bioluminescence intensity. The bioluminescent intensity in the mouse spleens was  
185 quantified using the LivingImage 4.0 software package and reported as photon  
186 counts/second.

187 *Flow cytometric analysis for the evaluation of cellular phenotype and perforin and*  
188 *granzyme B expression.* Splenocytes isolated from the mice were stained with APC-  
189 labeled anti-human CD45 monoclonal antibody (mAb), FITC-labeled anti-human CD3  
190 mAb, phycoerythrin (PE)-Cy7-labeled anti-human CD4, Pacific Blue-labeled anti-human  
191 CD8 mAb, PE-labeled anti-human CD56/CD16 mAb and APC-labeled anti-human  
192 CD16 mAb (all from BioLegend, San Diego, CA) and were analyzed using an LSRII (BD  
193 Biosciences, San Jose, CA) and FlowJo software (Treestar, Ashland, OR) as described  
194 (24). The effect of IL-15 superagonist treatment on perforin and granzyme B expression  
195 in NK cells was determined by treating human PBMCs from seronegative donors with  
196 the indicated concentration of IL-15 superagonist for two days. The PBMCs were  
197 washed, stained with APC-CY7-labeled anti-human CD3 mAb and PE-labeled anti-

198 human CD56 mAb, incubated in fixation and permeabilization buffers, intracellularly  
199 stained with FITC-conjugated anti-human granzyme B mAb and with PerCP-Cy5.5-  
200 labeled perforin (BioLegend) and washed. The mean fluorescent intensity (MFI:  
201 geometric mean) of granzyme B and perforin expression by the gated CD3<sup>+</sup>CD56<sup>+</sup> NK  
202 cells was determined by analysis on a FACSverse with FACSuite software (BD  
203 Biosciences).

204

205 *Measurement of NK cell cytotoxic function directed against K562 cells and HIV-1-*  
206 *infected ACH2 cells.* The capacity of the IL-15 superagonist treatment to stimulate NK  
207 cell degranulation was examined by quantifying expression of CD107a using flow  
208 cytometry after incubation of PBMCs harvested from HIV-negative donors with K562  
209 cells as described (27). In parallel, we determined the effect of IL-15 superagonist  
210 stimulation on the functional cytolytic activity of NK cells by quantifying their capacity to  
211 lyse K562 target cells using a modification of a published technique (28). Briefly, K562  
212 cells target cells were labeled with CellTrace<sup>TM</sup> Violet (Invitrogen-Life Technologies,  
213 Grand Island, NY). Human PBMCs either untreated or treated with the IL-15  
214 superagonist (10 nM) were mixed with CellTrace<sup>TM</sup> Violet-labeled K562 target cells at  
215 the indicated effector:target (E:T) ratio in complete media and incubated at 37°C with  
216 5% CO<sub>2</sub> for 3 days. The K562 target cell viability was assessed by analysis of  
217 propidium iodide positive staining of the CellTrace<sup>TM</sup> Violet-labeled K562 target cells on  
218 a BD FACSVerse and cytotoxicity was calculated as the percentage of dead target cells  
219 in samples co-cultured with effector cells.

220 To determine the capacity of the IL-15 superagonist to stimulate NK cell-  
221 mediated lysis of HIV-1-infected cells, PBMCs were harvested from HIV-negative  
222 donors and cultured ( $5 \times 10^5$  cells/well) with the indicated concentration of the IL-15  
223 superagonist for 2 days. ACH2 cells, T cells latently infected with a single integrated  
224 HIV-1 provirus which display minimal HIV-1 replication unless stimulated with PMA  
225 and/or TNF $\alpha$ , were obtained through the NIH AIDS Reagent Program, Division of AIDS,  
226 NIAID, NIH (29). ACH2 cells were used as target cells and were either not activated or  
227 were stimulated with PMA (2 ng/ml) and TNF $\alpha$  (2 ng/ml) for 24 hours to stimulate HIV-1  
228 production as described (30). After the effector cells were cultured for 48 hours with the  
229 indicated dose of the IL-15 superagonist, the effector cells were co-cultured with  
230 unactivated or activated ACH2 cells at an E:T ratio of 25:1 for 24 hours as described  
231 (31). Lysis of target cells was then measured using the fluorescence-based CytoTox-  
232 One Homogeneous Membrane Integrity Assay (Promega) according to the  
233 manufacturer's instructions. Background fluorescence was determined by adding  
234 unstimulated target ACH2 cells ( $2 \times 10^4$  cells/well) to effector PBMCs ( $5 \times 10^5$  cells/well)  
235 that were either treated or untreated with the IL-15 superagonist at an E:T ratio of 25:1.  
236 The percent of specific cell lysis was determined by subtracting background fluorescence  
237 from experimental fluorescence and dividing by the maximum LDH release from target  
238 cells, determined by lysing ( $2 \times 10^4$  cells/well) stimulated ACH2 cells, and then  
239 multiplying the resulting number by 100.

240 *Statistical analysis of data.* GraphPad Prism statistical software was used for  
241 statistical analysis with an independent two-tailed Students *t*-test. Differences were  
242 considered statistically different for *P* values < 0.05.

243            *Study approval.* All the studies were performed under protocols approved by the  
244 Institute for Animal Studies and the Institutional Review Board at the Albert Einstein  
245 College of Medicine in compliance with the human and animal experimentation  
246 guidelines of the United States Department of Health and Human Services.

247

## 248 **Results**

249            *The in vitro cytolytic activity of human NK cells is induced by IL-15 superagonist*  
250 *treatment.* The IL-15 superagonist, IL-15N72D:IL-15R $\alpha$ Su/Fc, is a homodimer of two  
251 engineered IgG1 Fc domains fused with the IL-15R $\alpha$  binding domain each of which is  
252 bound to a mutated IL-15 molecule, IL-15N72D, which activates IL-15R $\beta\gamma$  chain-  
253 expressing NK cells by mimicking the trans-presentation of IL-15 by the soluble IL-15:IL-  
254 15R $\alpha$  complex (Figure 1A). Based on its capacity to potently activate the cytotoxic  
255 activity of NK cells and CD8<sup>+</sup> T cells, this IL-15 superagonist, also identified as ALT-803,  
256 has shown promise as an immunostimulatory agent to treat cancer (32). We  
257 investigated whether activation of NK cells by treatment with this IL-15 superagonist  
258 would increase their cytotoxic activity to enable them to eliminate HIV-1 infected cells  
259 and inhibit the *in vivo* acquisition of HIV-1 infection. The predominant killing pathway  
260 utilized by NK cells to kill target cells they identify as malignant or infected is by  
261 exocytosis of preformed granules containing lytic proteins, mainly perforin and  
262 granzyme B, into a cytotoxic synapse formed with the target cells (33). Because  
263 increasing cellular levels of perforin and granzyme B increases the cytotoxic capacity of  
264 NK cells (34), we examined whether IL15R-agonist treatment increased the cytolytic  
265 capacity of NK cells by inducing perforin and granzyme B production. Human PBMCs

266 from six seronegative donors were treated with the IL-15 superagonist or untreated for  
267 two days and then analyzed by flow cytometry to quantify the intracellular expression of  
268 perforin and granzyme B by the NK cells. As compared to NK cells in the untreated  
269 PBMCs, the NK cells in the human PBMCs treated with the IL15R-agonist for two days  
270 displayed significantly higher levels of perforin (Figure 1B) and significantly higher levels  
271 of granzyme B (Figure 1C) in a dose responsive fashion. CD107a is a marker of NK cell  
272 degranulation, and its upregulation on cell surfaces is induced by interaction with MHC-  
273 negative target cells and correlates with NK cell lysis of target cells and cytokine  
274 secretion (27). To evaluate the capacity of IL-15 superagonist-stimulation to increase  
275 the cytolytic activity of NK cells, we incubated human PBMCs isolated from  
276 seronegative donors with K562 cells, a highly sensitive *in vitro* target for NK cells, and  
277 examined the effect of treatment with the IL-15 superagonist on NK cell-surface-  
278 expression of CD107a. In the absence of K562 cells, incubation of the PBMCs with the  
279 IL-15 superagonist (1,000 pM) did not significantly increase cell-surface CD107a  
280 expression by the NK cells (~5% CD107a positive, data not shown). When the PBMCs  
281 were incubated with the target K562 cells, cell-surface CD107a expression increased by  
282 5-fold (~26%), and treatment of the PBMCs with the IL-15 superagonist significantly  
283 increased their cell-surface CD107a expression by an additional 2.3-fold (~62%) in a  
284 dose responsive manner (Figure 1D). Increased cell-surface expression of CD107a  
285 induced by treatment the IL-15 superagonist was associated with an increase in the *in*  
286 *vitro* capacity of the NK cells in the PBMCs to lyse K562 cells (Figure 1E), the standard  
287 NK-sensitive target cell for human NK cell assays (28). In addition, NK cell stimulation  
288 by IL-15 superagonist was also indicated by its induction of the early activation marker

289 CD69 (data not shown). Taken together, these data demonstrate that the IL-15  
290 superagonist enhances the *in vitro* cytotoxic capability of human NK cells, possibly via  
291 upregulating their expression of the effector molecules granzyme B and perforin and  
292 increasing their activation state.

293 To determine whether IL-15 superagonist-stimulation increased the capacity of  
294 NK cells to kill HIV-1-infected cells, we used ACH2 cells, a latently infected cell line that  
295 can be induced to produce HIV-1 after PMA and/or TNF- $\alpha$  treatment (29) and which has  
296 previously been used as target cells to evaluate HIV-1-specific NK cell-mediated ADCC  
297 activity (31). Unstimulated PMBCs and IL-15 superagonist-stimulated PMBCs were  
298 incubated with unactivated ACH2 cells or PMA/TNF- $\alpha$ -stimulated ACH2 cells and lysis  
299 of ACH2 cells was quantified by measuring the amount of LDH released into the culture  
300 supernatant. Human PMBCs treated with the IL-15 superagonist (100 nM) displayed a  
301 ~8-fold increased lysis of stimulated ACH2 cells ( $p < 0.0001$ ) as compared to  
302 unstimulated PMBCs (Figure 1F).

303 *In vivo* HIV-1 infection is potently suppressed by treatment of hu-spl-PBMC-NSG  
304 mice with the IL-15 superagonist. We next examined whether the increased *in vitro* NK  
305 cell cytotoxic activity induced by the IL-15 superagonist correlated with an increased  
306 capacity of IL-15 superagonist-activated NK cells to inhibit acute *in vivo* HIV-1 infection.  
307 For these studies we used a humanized mouse model that supports *in vivo* HIV-1  
308 infection, hu-spl-PBMC-NSG mice, NSG mice intrasplenically injected with human  
309 PMBCs, which we previously used to evaluate HIV-1-specific CD8<sup>+</sup> T cell activity (25).  
310 The spleens of these mice continue to be populated with human PMBCs including NK  
311 cells and support HIV-1 infection for at least 1 month after intrasplenic injection. This

312 model also permits us to identify effector cells responsible for anti-HIV-1 activity by  
313 removing specific cell populations from the human PBMCs prior to intrasplenically  
314 injecting them into the mouse spleens. As the infectious inoculum, we used HIV-LucR, a  
315 replication-competent molecular HIV clone expressing the HIV-1<sub>JR-CSF</sub> Env protein and a  
316 *Renilla* luciferase reporter gene, which enables HIV-1 infection to be quantified by  
317 directly measuring the luciferase activity of the infected cells (21). HIV-LucR virus has  
318 been well-established as an infectious inoculum that can be used to evaluate the  
319 capacity of antibodies, NK cells and CD8 T cells to inhibit HIV-1 infection (35-42). One  
320 day after hu-spl-PBMC-NSG mice were infected with HIV-1 by intrasplenic injection with  
321 HIV-LucR, one group of mice was intravenously injected with a dose of the IL-15  
322 superagonist. Five days later, HIV-1 infection was quantified by determining the level of  
323 expression of the luciferase reporter gene in the mouse spleens. Splenic lysates of the  
324 IL-15 superagonist-treated mice displayed a greater than 99% reduction in luciferase  
325 activity (average = 804 RLU) as compared to untreated mice (average = 827,829 RLU),  
326 indicating that the IL-15 superagonist treatment delivered one day after direct  
327 intrasplenic challenge with HIV-1 significantly suppressed ( $p < 0.001$ ) acute HIV-1  
328 infection (Figure 2A). The use of an infectious HIV-1 expressing a LucR reporter gene  
329 enabled us to directly visualize *in vivo* infection by intravital bioluminescent imaging and  
330 observe suppression of acute HIV-1 infection by activation of NK cells by the IL-15  
331 superagonist. Hu-spl-PBMC-NSG mice were infected with HIV-1 by intrasplenic  
332 injection with HIV-LucR. One day later the mice were treated either with the IL-15  
333 superagonist or PBS and four days later, the level of *in vivo* HIV-1 infection was  
334 visualized and quantified by bioluminescent imaging of LucR activity using the IVIS

335 Spectrum intravital imaging system. Direct visualization demonstrated that the level of  
336 bioluminescence in the spleens of the IL-15 superagonist-treated hu-spl-PBMC-NSG  
337 mice was markedly reduced in the IL-15 superagonist-treated hu-spl-PBMC-NSG mice  
338 as compared to untreated mice (Figure 2B). Quantification of the bioluminescent signal  
339 by measurement of total photon flux demonstrated that IL-15 superagonist treatment  
340 significantly reduced bioluminescence due to HIV-LucR infection (Figure 2C).

341 To examine the effect of acute HIV-1 infection and treatment with IL-15  
342 superagonist on the human T cell and NK cell populations in the hu-spl-PBMC-NSG  
343 mouse spleens, one group of hu-spl-PBMC-NSG mice were inoculated with HIV-LucR  
344 and one day later some of the HIV-LucR-inoculated mice and HIV-LucR-uninoculated  
345 mice were intravenously injected with a dose of the IL-15 superagonist. Six days later,  
346 the human CD3<sup>-</sup>CD56<sup>+</sup> NK cell and CD3<sup>+</sup> T cell populations (Figure 3A) and CD4<sup>+</sup> and  
347 CD8<sup>+</sup> T cell populations (Figure 3B) in the mouse spleens were evaluated by flow  
348 cytometry. These results demonstrated that one week after intrasplenic injection, the  
349 hu-spl-PBMC-NSG mouse spleens were well-populated with human NK cells, CD4<sup>+</sup> T  
350 cells and CD8<sup>+</sup> T cells which was not markedly altered as a consequence of HIV-LucR-  
351 inoculation or IL-15 superagonist treatment.

352 We next investigated whether activation of NK cells by the IL-15 superagonist  
353 could inhibit the acquisition of HIV-1 infection even when the NK cells were activated by  
354 IL-15 superagonist administered three days after inoculation with HIV-1. Hu-spl-PBMC-  
355 NSG mice were intrasplenically challenged with HIV-LucR and three days later some  
356 mice were treated with a dose of the IL-15 superagonist. Five days after treatment, the  
357 level of HIV-1 infection in the hu-spl-PBMC-NSG mouse spleens was quantified and

358 was significantly reduced ( $p < 0.005$ ) in the IL-15 superagonist-treated mice by almost  
359 95% as compared to untreated mice (Figure 4A). We extended those findings by  
360 examining whether the potent suppressive effect mediated by IL-15 superagonist  
361 treatment was sustained by quantifying the level of HIV-1 infection in the mouse spleens  
362 at 2 weeks and at 3 weeks after treatment. When hu-spl-PBMC-NSG mice were treated  
363 three days after intrasplenic injection with HIV-LucR with an intravenous injection of the  
364 IL-15 superagonist, the development of HIV-1 infection in the humanized mouse  
365 spleens was significantly inhibited ( $p < 0.05$ ) by greater than 90% when evaluated at day  
366 14 and 21 post-treatment as compared to untreated mice (Figure 4B). The continued  
367 reduction in the level of HIV-1 infection by over 97% at 21 days after inoculation  
368 suggested that IL-15 superagonist treatment initiated 3 days after HIV-1 inoculation  
369 eliminated cells initially infected with HIV-1 and thereby potentially suppressed the  
370 establishment of primary HIV-1 infection. However, when activation of NK cells by the  
371 IL-15 superagonist is delayed by not initiating IL-15 superagonist treatment until 5 days  
372 after HIV-1 inoculation, establishment of primary HIV-1 infection was no longer  
373 significantly inhibited (data not shown).

374 *NK cells mediate IL-15 superagonist-induced inhibition of in vivo HIV-1 infection.*

375 To confirm that NK cells activated by the IL-15 superagonist were responsible for  
376 inhibiting *in vivo* HIV-1 infection, we depleted by immunomagnetic sorting either the  
377 population of CD8<sup>+</sup> T cells or the population of NK cells from the PBMC prior to  
378 intrasplenic injection (Figure 5A). NSG mice were intrasplenically injected with either  
379 activated unfractionated PBMCs, CD8<sup>+</sup> T cell-depleted PBMCs, or NK cell-depleted  
380 PBMCs and in parallel infected with HIV-1 by intrasplenic injection with HIV-LucR. One

381 day later, some groups of mice were either untreated or treated with one intravenous  
382 dose of the IL-15 superagonist and five days later the level of acute HIV-1 infection was  
383 quantified by determining the level of expression of the luciferase reporter gene in the  
384 mouse splenocytes. While the depletion of CD8<sup>+</sup> T cells from the PBMCs had only  
385 minimal effects on reducing the IL-15 superagonist-mediated inhibition of HIV-1  
386 infection, NK cell-depletion of human PBMCs completely abrogated ( $p < 0.0001$ ) IL-15  
387 superagonist-mediated inhibition of *in vivo* HIV-1 infection (Figure 5B).

388 *Human NK cells activated by in vivo IL-15 superagonist treatment eliminate HIV-*  
389 *1 infected cells in hu-spl-PBMC-NSG mouse spleens.* To determine whether treatment  
390 with the IL-15 superagonist during acute HIV-1 infection induced *in vivo* activation of  
391 human NK cells in the hu-spl-PBMC-NSG, we examined its effect on expression of  
392 CD69, a functional marker for NK cell activation that correlates with the expression of  
393 the degranulation marker, CD107a (43, 44). Hu-spl-PBMC-NSG mice were infected with  
394 HIV-1 by intrasplenic injection with HIV-LucR. One day later, one group of mice was  
395 treated with the IL-15 superagonist. Two days after IL-15 superagonist treatment, flow  
396 cytometric analysis demonstrated that the CD3<sup>+</sup>/CD56<sup>+</sup>/CD16<sup>+</sup> human NK cells in the  
397 spleens of humanized mice displayed an almost three-fold increase ( $p < 0.001$ ) in CD69  
398 expression as compared to human NK cells in spleen of untreated hu-spl-PBMC-NSG  
399 mice (Figure 6). We next investigated whether *in vivo* IL-15 superagonist activation of  
400 NK cells increased their capacity to kill HIV-1-infected cells in hu-spl-PBMC-NSG mice  
401 with established *in vivo* infection. Hu-spl-PBMC-NSG mice were infected by intrasplenic  
402 injection of HIV-LucR. After five days, which provided sufficient time for *in vivo* infection  
403 to develop, one group of mice was treated with an intravenous injection of the IL-15

404 superagonist. One day after IL-15 superagonist treatment, the level of HIV-1 infection in  
405 the mouse spleens, as determined by measurement of LucR activity, was reduced by  
406 greater than 90%, as compared to LucR levels in the spleens of untreated mice (Figure  
407 7). Taken together, these results indicated that *in vivo* treatment with an IL-15  
408 superagonist activated human NK cells, which increased their *in vivo* cytolytic activity  
409 and enabled them to kill HIV-1-infected cells and suppress acute HIV-1 infection.

410

#### 411 **Discussion**

412 To our knowledge, this study is the first reported demonstration that *in vivo*  
413 activation of NK cells can inhibit acute HIV-1 infection. The NK cells were activated by  
414 *in vivo* treatment with a superagonist of IL-15, a multifunctional cytokine which plays a  
415 crucial role in NK cell and CD8<sup>+</sup> T cell development, activation, proliferation,  
416 differentiation and functional activity (12, 15, 45). PBMCs treated *in vitro* with the IL-15  
417 superagonist displayed increased NK cell activity as indicated by their increased  
418 expression of perforin and granzyme B as well as cell-surface CD107a upon exposure  
419 to K562 cells and by their augmented capacity to lyse K562 cells, an NK cell-sensitive  
420 target, and activated ACH2 cells, an HIV-1 producing T cell line. Activation of the human  
421 NK cells by *in vivo* treatment with the IL-15 superagonist after intrasplenic injection of  
422 human PBMCs into the NSG mice was indicated by their increased expression of CD69,  
423 a marker associated with NK cell activation (43, 44). Acute *in vivo* HIV-1 infection was  
424 potently inhibited by IL-15 superagonist treatment of NSG mice intrasplenically injected  
425 with unfractionated human PBMCs or with CD8<sup>+</sup> T cell-depleted PBMCs. In contrast,  
426 when NK cells were depleted from the human PBMCs prior to their intrasplenic injection

427 into the NSG mice, acute HIV-1 infection was not inhibited by treatment with the IL-15  
428 superagonist. This demonstrated that human NK cells were the crucial effector cells  
429 activated by *in vivo* treatment with the IL-15-agonist that mediated inhibition of acute *in*  
430 *vivo* HIV-1 infection. Taken together, our data indicate that *in vivo* activation of human  
431 NK cells by treatment with the IL-15 superagonist, even when delayed until 3 days after  
432 HIV-1 inoculation, suppressed the establishment of productive infection. It is likely that  
433 this is due to NK cell-mediated elimination of a large fraction of the cells initially infected  
434 with HIV-1 during the acute infection, which markedly reduced the population of HIV-1-  
435 infected cells and subsequent level of productive HIV-1 infection. This was supported by  
436 our demonstration that one day after treatment with the IL-15 superagonist, the level of  
437 HIV-1 infection in the spleens of hu-spl-PBMC-NSG mice with established HIV-1  
438 infection was reduced by greater than 90%. While treatment with the IL-15 superagonist  
439 initiated 5 days after inoculation markedly reduced the number of HIV-1-infected cells  
440 measured one day later (i.e. measured at day 6 after inoculation as shown in Figure 7),  
441 sustained suppression of infection was not observed in these mice as it was in mice  
442 treated with the IL-15 superagonist within 3 days after inoculation. This decline in  
443 sustainable inhibition of HIV-1 infection may be due to the additional two-day deferral in  
444 treatment which provides HIV-1 with more time to spread sufficiently to a critical number  
445 of infected cells that escape NK cell-mediated killing and disseminate infection. Thus,  
446 administration of the IL-15 superagonist at day 3 or day 5 after inoculation can potentially  
447 inhibit HIV infection, but sustained suppression of HIV infection only occurs when the IL-  
448 15 superagonist is administered within 3 days of exposure. NK cells contribute to the  
449 control of HIV-1 replication in HIV-1-infected individuals as indicated by the capacity of

450 HLA-B Bw4-80I-activated NK cells that express the activating killer immunoglobulin-like  
451 NK cell receptor (KIR3DS1) to potently inhibit HIV-1 replication (46) and the delayed  
452 progression of HIV-1 disease observed in individuals expressing HLA-B Bw4-80I, the  
453 ligand for KIR3DL1 receptors which are highly expressed on NK cells (47). NK cells  
454 constitutively express inhibitory and activating receptors capable of identifying and  
455 rapidly lysing virally infected cells (48). Consequently, even during initial exposure to  
456 HIV-1 and prior to the development of HIV-specific adaptive immune responses, NK  
457 cells can recognize and eliminate HIV-1 infected cells whose HLA Class I MHC  
458 molecules are downregulated by HIV-1 Nef (48). The capacity of some NK cells to  
459 recognize and kill HIV-1-infected cells may be limited by the selective Nef-mediated  
460 reduction of only HLA-A and HLA-B molecules with continued expression of HLA-C and  
461 HLA-E molecules (49). It is possible that IL-15 superagonist treatment may activate  
462 other NK cells which are capable of effectively killing HIV-infected CD4<sup>+</sup> T cells despite  
463 their continued expression of HLA-C and HLA-E because this subpopulation of NK cells  
464 does not express inhibitory receptors specific for HLA-C and HLA-E molecules (11).  
465 Activated NK cells may also identify and kill HIV-1 infected cells by alternative  
466 mechanisms including the detection of stress molecules whose expression is induced  
467 by viral infection (50, 51). In addition, activated NK cells may also inhibit the spread of  
468 acute HIV-1 infection by secreting CC chemokines, such as RANTES, MIP1- $\alpha$  and  
469 MIP1- $\beta$ , which block HIV-1 binding to CCR5 (52).

470         These results extend the reports of previous studies which first suggested a role  
471 for IL-15 in treating HIV-1 infection based on its capacity to potently activate CD8<sup>+</sup> T  
472 cells and NK cells (53), enhance the *in vitro* function and survival of HIV-specific CD8<sup>+</sup> T

473 cells (54), delay recurrence of HIV-1 viremia after antiretroviral therapy interruption (55)  
474 and prevent HIV-1 transmission during breast feeding (56). While IL-15-induced  
475 stimulation of NK cells and CD8<sup>+</sup> T cells may have the beneficial effect of inhibiting HIV-  
476 1 replication during acute infection as shown in our study, during chronic infection IL-15-  
477 mediated activation of CD4<sup>+</sup> T cells may potentially have the opposite and deleterious  
478 effect of increasing their susceptibility to HIV-1 infection. This was indicated in studies of  
479 acutely SIV-infected macaques treated with IL-15 whose memory CD4<sup>+</sup> T cells  
480 displayed increased susceptibility to SIV infection (57) and who subsequently displayed  
481 increased viral set points and accelerated progression of disease (58). It is possible that  
482 our observation that the IL-15 superagonist potently inhibited HIV-1 infection in the hu-  
483 spl-PBMC-NSG mice is due to its ~25-fold higher biological activity and >35-fold longer  
484 serum half-life than soluble IL-15 (20). The greater potency of the IL-15 superagonist  
485 as compared to IL-15 may enable it to stimulate a more potent anti-HIV-1-immune  
486 response than the recombinant IL-15 used to treat the macaques and outweigh the  
487 potential deleterious effect of IL-15-mediated activation of CD4<sup>+</sup> T cells, particularly  
488 during acute infection. It is also possible that IL-15, particularly when delivered as a  
489 complex with the IL-15R $\alpha$  chain, has different effects on macaque NK cells and T cells  
490 than on human NK cells and T cells.

491 Multiple studies have demonstrated that immunostimulation of CD8<sup>+</sup> T cells and  
492 NK cells by the IL-15:IL-15R $\alpha$  complex stimulates the *in vivo* clearance of tumors and  
493 has led to the initiation of Phase I trials for their use to treat cancer (59). While studies in  
494 mice have indicated that CD8<sup>+</sup> T cells were the crucial effector cells mediating IL-15-  
495 induced clearance of tumors (20, 60), our results demonstrate that activated NK cells

496 were the crucial effector cells activated by the IL-15 superagonist to inhibit acute HIV-1  
497 infection. The functional activity of NK cells is impaired during chronic HIV-1 infection  
498 (9), and it is possible that this impairment may be reversed by treatment with the IL-15  
499 superagonist. Further studies in humanized mice infected with HIV-1 and treated with  
500 the IL-15 superagonist, should enable us to further delineate the effects of NK cell  
501 activation mediated by IL-15 superagonist treatment on inhibiting *in vivo* HIV-1 infection.  
502 Treatment of SHIV-infected monkeys with broadly neutralizing HIV-specific antibodies  
503 improved the function of their HIV-specific CD8<sup>+</sup> T cells and lowered their viral-load set  
504 points, suggesting that neutralizing antibody therapy could increase anti-viral immune  
505 responses to enable better control of SHIV infection (61). It is possible that NK cell-  
506 mediated antibody-dependent cellular cytotoxicity (ADCC) may contribute to the  
507 reported reduction in rebound viremia in humanized mice treated with broadly  
508 neutralizing HIV-specific antibodies (62). Thus, an intriguing possibility is that increasing  
509 NK cell activity by treatment with the IL-15 superagonist may further facilitate the anti-  
510 HIV-1 activity of neutralizing antibody therapy by augmenting ADCC activity. Further  
511 studies in humanized mice infected with HIV-1 and treated with the IL-15 superagonist,  
512 should enable us to further delineate the effects of IL15R-agonist-mediated NK cell  
513 activation on directly inhibiting *in vivo* HIV-1 infection and further suppressing HIV-1  
514 infection through ADCC when combined with broadly neutralizing HIV-specific antibody  
515 therapy.  
516  
517

518 **Acknowledgments**

519 This work was supported by the National Institute of Drug Abuse at the National  
520 Institutes of Health (DA033788), the Einstein-Montefiore Center for AIDS Research  
521 (P30-AI51519), the UAB Center for AIDS Research (P30-AI277670), the National  
522 Institute of Allergy and Infectious Diseases at the National Institutes of Health (T32-  
523 AI007501 to K.S. and C.C.), NIH Center for HIV-1/AIDS Vaccine Immunology (CHAVI)  
524 (UO1-AI067854 to J.C.K. and C.O.), the Charles Michael Chair in Autoimmune  
525 Diseases (to HG), and a VHA Merit Review Award (to J.C.K.). Altor BioScience  
526 Corporation provided funds to support some of the costs for purchasing, housing,  
527 infecting and analyzing the mice. Kieran Seay, Candice Church, Jian Hua Zheng,  
528 Kathryn Deneroff, Christina Ochsenbauer and John C. Kappes report no potential  
529 conflicts of interest. Hing C. Wong, Emily K. Jeng and Bai Liu are employees and  
530 stockholders of Altor BioScience Corporation which provided the IL-15 superagonist,  
531 ALT-803.

532

533 **References**

- 534 1. **Walker BD, Yu XG.** 2013. Unravelling the mechanisms of durable control of HIV-  
535 1. *Nat Rev Immunol* **13**:487-498.
- 536 2. **Johnston MI, Fauci AS.** 2007. An HIV vaccine--evolving concepts. *N Engl J*  
537 *Med* **356**:2073-2081.
- 538 3. **Mellors JW, Kingsley LA, Rinaldo CR, Jr., Todd JA, Hoo BS, Kokka RP,**  
539 **Gupta P.** 1995. Quantitation of HIV-1 RNA in plasma predicts outcome after  
540 seroconversion. *Ann Intern Med* **122**:573-579.
- 541 4. **Mellors JW, Rinaldo CR, Jr., Gupta P, White RM, Todd JA, Kingsley LA.**  
542 1996. Prognosis in HIV-1 infection predicted by the quantity of virus in plasma.  
543 *Science* **272**:1167-1170.
- 544 5. **Lodi S, Meyer L, Kelleher AD, Rosinska M, Ghosn J, Sannes M, Porter K.**  
545 2012. Immunovirologic control 24 months after interruption of antiretroviral  
546 therapy initiated close to HIV seroconversion. *Arch Intern Med* **172**:1252-1255.
- 547 6. **Saez-Cirion A, Bacchus C, Hocqueloux L, Avettand-Fenoel V, Girault I,**  
548 **Lecuroux C, Potard V, Versmisse P, Melard A, Prazuck T, Descours B,**  
549 **Guergnon J, Viard JP, Boufassa F, Lambotte O, Goujard C, Meyer L,**  
550 **Costagliola D, Venet A, Pancino G, Autran B, Rouzioux C.** 2013. Post-  
551 treatment HIV-1 controllers with a long-term virological remission after the  
552 interruption of early initiated antiretroviral therapy ANRS VISCONTI Study. *PLoS*  
553 *Pathog* **9**:e1003211.
- 554 7. **Salgado M, Rabi SA, O'Connell KA, Buckheit RW, 3rd, Bailey JR, Chaudhry**  
555 **AA, Breaud AR, Marzinke MA, Clarke W, Margolick JB, Siliciano RF,**

- 556 **Blankson JN.** 2011. Prolonged control of replication-competent dual- tropic  
557 human immunodeficiency virus-1 following cessation of highly active antiretroviral  
558 therapy. *Retrovirology* **8**:97.
- 559 8. **Alter G, Teigen N, Ahern R, Streeck H, Meier A, Rosenberg ES, Altfeld M.**  
560 2007. Evolution of innate and adaptive effector cell functions during acute HIV-1  
561 infection. *J Infect Dis* **195**:1452-1460.
- 562 9. **Naranbhai V, Altfeld M, Karim SS, Ndung'u T, Karim QA, Carr WH.** 2013.  
563 Changes in Natural Killer cell activation and function during primary HIV-1  
564 Infection. *PLoS One* **8**:e53251.
- 565 10. **Jost S, Altfeld M.** 2013. Control of human viral infections by natural killer cells.  
566 *Annu Rev Immunol* **31**:163-194.
- 567 11. **Bonaparte MI, Barker E.** 2004. Killing of human immunodeficiency virus-infected  
568 primary T-cell blasts by autologous natural killer cells is dependent on the ability  
569 of the virus to alter the expression of major histocompatibility complex class I  
570 molecules. *Blood* **104**:2087-2094.
- 571 12. **Liu K, Catalfamo M, Li Y, Henkart PA, Weng NP.** 2002. IL-15 mimics T cell  
572 receptor crosslinking in the induction of cellular proliferation, gene expression,  
573 and cytotoxicity in CD8+ memory T cells. *Proc Natl Acad Sci U S A* **99**:6192-  
574 6197.
- 575 13. **Lucas M, Schachterle W, Oberle K, Aichele P, Diefenbach A.** 2007. Dendritic  
576 cells prime natural killer cells by trans-presenting interleukin 15. *Immunity*  
577 **26**:503-517.

- 578 14. **Mortier E, Woo T, Advincula R, Gozalo S, Ma A.** 2008. IL-15Ralpha  
579 chaperones IL-15 to stable dendritic cell membrane complexes that activate NK  
580 cells via trans presentation. *J Exp Med* **205**:1213-1225.
- 581 15. **Waldmann TA.** 2006. The biology of interleukin-2 and interleukin-15:  
582 implications for cancer therapy and vaccine design. *Nat Rev Immunol* **6**:595-601.
- 583 16. **Chertova E, Bergamaschi C, Chertov O, Sowder R, Bear J, Roser JD, Beach  
584 RK, Lifson JD, Felber BK, Pavlakis GN.** 2013. Characterization and favorable  
585 in vivo properties of heterodimeric soluble IL-15. IL-15Ralpha cytokine compared  
586 to IL-15 monomer. *J Biol Chem* **288**:18093-18103.
- 587 17. **Bergamaschi C, Bear J, Rosati M, Beach RK, Alicea C, Sowder R, Chertova  
588 E, Rosenberg SA, Felber BK, Pavlakis GN.** 2012. Circulating IL-15 exists as  
589 heterodimeric complex with soluble IL-15Ralpha in human and mouse serum.  
590 *Blood* **120**:e1-8.
- 591 18. **Wei X, Orchardson M, Gracie JA, Leung BP, Gao B, Guan H, Niedbala W,  
592 Paterson GK, McInnes IB, Liew FY.** 2001. The Sushi domain of soluble IL-15  
593 receptor alpha is essential for binding IL-15 and inhibiting inflammatory and  
594 allogenic responses in vitro and in vivo. *J Immunol* **167**:277-282.
- 595 19. **Zhu X, Marcus WD, Xu W, Lee HI, Han K, Egan JO, Yovandich JL, Rhode  
596 PR, Wong HC.** 2009. Novel human interleukin-15 agonists. *J Immunol* **183**:3598-  
597 3607.
- 598 20. **Xu W, Jones M, Liu B, Zhu X, Johnson CB, Edwards AC, Kong L, Jeng EK,  
599 Han K, Marcus WD, Rubinstein MP, Rhode PR, Wong HC.** 2013. Efficacy and  
600 mechanism-of-action of a novel superagonist interleukin-15: interleukin-15

- 601 receptor alphaSu/Fc fusion complex in syngeneic murine models of multiple  
602 myeloma. *Cancer Res* **73**:3075-3086.
- 603 21. **Edmonds TG, Ding H, Yuan X, Wei Q, Smith KS, Conway JA, Wieczorek L,**  
604 **Brown B, Polonis V, West JT, Montefiori DC, Kappes JC, Ochsenbauer C.**  
605 2010. Replication competent molecular clones of HIV-1 expressing Renilla  
606 luciferase facilitate the analysis of antibody inhibition in PBMC. *Virology* **408**:1-  
607 13.
- 608 22. **Miyawaki A.** 2007. Bringing bioluminescence into the picture. *Nat Methods*  
609 **4**:616-617.
- 610 23. **Han KP, Zhu X, Liu B, Jeng E, Kong L, Yovandich JL, Vyas VV, Marcus WD,**  
611 **Chavillaz PA, Romero CA, Rhode PR, Wong HC.** 2011. IL-15:IL-15 receptor  
612 alpha superagonist complex: high-level co-expression in recombinant  
613 mammalian cells, purification and characterization. *Cytokine* **56**:804-810.
- 614 24. **Sango K, Joseph A, Patel M, Osiecki K, Dutta M, Goldstein H.** 2010. Highly  
615 active antiretroviral therapy potently suppresses HIV infection in humanized  
616 Rag2<sup>-/-</sup>gammac<sup>-/-</sup> mice. *AIDS Res Hum Retroviruses* **26**:735-746.
- 617 25. **Joseph A, Zheng JH, Follenzi A, Dilorenzo T, Sango K, Hyman J, Chen K,**  
618 **Piechocka-Trocha A, Brander C, Hooijberg E, Vignali DA, Walker BD,**  
619 **Goldstein H.** 2008. Lentiviral vectors encoding human immunodeficiency virus  
620 type 1 (HIV-1)-specific T-cell receptor genes efficiently convert peripheral blood  
621 CD8 T lymphocytes into cytotoxic T lymphocytes with potent in vitro and in vivo  
622 HIV-1-specific inhibitory activity. *J Virol* **82**:3078-3089.

- 623 26. **Seay K, Qi X, Zheng JH, Zhang C, Chen K, Dutta M, Deneroff K,**  
624 **Ochsenbauer C, Kappes JC, Littman DR, Goldstein H.** 2013. Mice transgenic  
625 for CD4-specific human CD4, CCR5 and cyclin T1 expression: a new model for  
626 investigating HIV-1 transmission and treatment efficacy. *PLoS One* **8**:e63537.
- 627 27. **Alter G, Malenfant JM, Altfeld M.** 2004. CD107a as a functional marker for the  
628 identification of natural killer cell activity. *J Immunol Methods* **294**:15-22.
- 629 28. **Zamai L, Mariani AR, Zauli G, Rodella L, Rezzani R, Manzoli FA, Vitale M.**  
630 1998. Kinetics of in vitro natural killer activity against K562 cells as detected by  
631 flow cytometry. *Cytometry* **32**:280-285.
- 632 29. **Folks TM, Clouse KA, Justement J, Rabson A, Duh E, Kehrl JH, Fauci AS.**  
633 1989. Tumor necrosis factor alpha induces expression of human  
634 immunodeficiency virus in a chronically infected T-cell clone. *Proc Natl Acad Sci*  
635 *U S A* **86**:2365-2368.
- 636 30. **Zhang T, Li Y, Wang YJ, Wang X, Young M, Douglas SD, Ho WZ.** 2007.  
637 Natural killer cell inhibits human immunodeficiency virus replication in chronically  
638 infected immune cells. *Antiviral Res* **73**:132-139.
- 639 31. **Perdomo MF, Levi M, Sallberg M, Vahlne A.** 2008. Neutralization of HIV-1 by  
640 redirection of natural antibodies. *Proc Natl Acad Sci U S A* **105**:12515-12520.
- 641 32. **Gomes-Giacoia E, Miyake M, Goodison S, Sriharan A, Zhang G, You L,**  
642 **Egan JO, Rhode PR, Parker AS, Chai KX, Wong HC, Rosser CJ.** 2014.  
643 Intravesical ALT-803 and BCG treatment reduces tumor burden in a carcinogen  
644 induced bladder cancer rat model; a role for cytokine production and NK cell  
645 expansion. *PLoS One* **9**:e96705.

- 646 33. **Leong JW, Fehniger TA.** 2011. Human NK cells: SET to kill. *Blood* **117**:2297-  
647 2298.
- 648 34. **Kim TD, Lee SU, Yun S, Sun HN, Lee SH, Kim JW, Kim HM, Park SK, Lee**  
649 **CW, Yoon SR, Greenberg PD, Choi I.** 2011. Human microRNA-27a\* targets  
650 Prf1 and GzmB expression to regulate NK-cell cytotoxicity. *Blood* **118**:5476-  
651 5486.
- 652 35. **Brown BK, Wieczorek L, Kijak G, Lombardi K, Currier J, Wesberry M,**  
653 **Kappes JC, Ngauy V, Marovich M, Michael N, Ochsenbauer C, Montefiori**  
654 **DC, Polonis VR.** 2012. The role of natural killer (NK) cells and NK cell receptor  
655 polymorphisms in the assessment of HIV-1 neutralization. *PLoS One* **7**:e29454.
- 656 36. **Chenine AL, Wieczorek L, Sanders-Buell E, Wesberry M, Towle T, Pillis DM,**  
657 **Molnar S, McLinden R, Edmonds T, Hirsch I, O'Connell R, McCutchan FE,**  
658 **Montefiori DC, Ochsenbauer C, Kappes JC, Kim JH, Polonis VR,**  
659 **Tovanabutra S.** 2013. Impact of HIV-1 backbone on neutralization sensitivity:  
660 neutralization profiles of heterologous envelope glycoproteins expressed in  
661 native subtype C and CRF01\_AE backbone. *PLoS One* **8**:e76104.
- 662 37. **deCamp A, Hraber P, Bailer RT, Seaman MS, Ochsenbauer C, Kappes J,**  
663 **Gottardo R, Edlefsen P, Self S, Tang H, Greene K, Gao H, Daniell X,**  
664 **Sarzotti-Kelsoe M, Gorny MK, Zolla-Pazner S, LaBranche CC, Mascola JR,**  
665 **Korber BT, Montefiori DC.** 2014. Global panel of HIV-1 Env reference strains  
666 for standardized assessments of vaccine-elicited neutralizing antibodies. *J Virol*  
667 **88**:2489-2507.

- 668 38. **McLinden RJ, Labranche CC, Chenine AL, Polonis VR, Eller MA, Wieczorek**  
669 **L, Ochsenbauer C, Kappes JC, Perfetto S, Montefiori DC, Michael NL, Kim**  
670 **JH.** 2013. Detection of HIV-1 neutralizing antibodies in a human  
671 CD4(+)/CXCR4(+)/CCR5(+) T-lymphoblastoid cell assay system. *PLoS One*  
672 **8:e77756.**
- 673 39. **Naarding MA, Fernandez N, Kappes JC, Hayes P, Ahmed T, Icyuz M,**  
674 **Edmonds TG, Bergin P, Anzala O, Hanke T, Clark L, Cox JH, Cormier E,**  
675 **Ochsenbauer C, Gilmour J.** 2014. Development of a luciferase based viral  
676 inhibition assay to evaluate vaccine induced CD8 T-cell responses. *J Immunol*  
677 *Methods* **409**:161-173.
- 678 40. **Ochsenbauer C, Edmonds TG, Ding H, Keele BF, Decker J, Salazar MG,**  
679 **Salazar-Gonzalez JF, Shattock R, Haynes BF, Shaw GM, Hahn BH, Kappes**  
680 **JC.** 2012. Generation of transmitted/founder HIV-1 infectious molecular clones  
681 and characterization of their replication capacity in CD4 T lymphocytes and  
682 monocyte-derived macrophages. *J Virol* **86**:2715-2728.
- 683 41. **Pace CS, Song R, Ochsenbauer C, Andrews CD, Franco D, Yu J, Oren DA,**  
684 **Seaman MS, Ho DD.** 2013. Bispecific antibodies directed to CD4 domain 2 and  
685 HIV envelope exhibit exceptional breadth and picomolar potency against HIV-1.  
686 *Proc Natl Acad Sci U S A* **110**:13540-13545.
- 687 42. **Sarzotti-Kelsoe M, Daniell X, Todd CA, Bilaska M, Martelli A, LaBranche C,**  
688 **Perez LG, Ochsenbauer C, Kappes JC, Rountree W, Denny TN, Montefiori**  
689 **DC.** 2014. Optimization and validation of a neutralizing antibody assay for HIV-1  
690 in A3R5 cells. *J Immunol Methods* **409**:147-160.

- 691 43. **Dons'koi BV, Chernyshov VP, Osypchuk DV.** 2011. Measurement of NK  
692 activity in whole blood by the CD69 up-regulation after co-incubation with K562,  
693 comparison with NK cytotoxicity assays and CD107a degranulation assay. *J*  
694 *Immunol Methods* **372**:187-195.
- 695 44. **Shah AH, Sowrirajan B, Davis ZB, Ward JP, Campbell EM, Planelles V,**  
696 **Barker E.** 2010. Degranulation of natural killer cells following interaction with  
697 HIV-1-infected cells is hindered by downmodulation of NTB-A by Vpu. *Cell Host*  
698 *Microbe* **8**:397-409.
- 699 45. **Soudja SM, Ruiz AL, Marie JC, Lauvau G.** 2012. Inflammatory monocytes  
700 activate memory CD8(+) T and innate NK lymphocytes independent of cognate  
701 antigen during microbial pathogen invasion. *Immunity* **37**:549-562.
- 702 46. **Alter G, Martin MP, Teigen N, Carr WH, Suscovich TJ, Schneidewind A,**  
703 **Streeck H, Waring M, Meier A, Brander C, Lifson JD, Allen TM, Carrington**  
704 **M, Altfeld M.** 2007. Differential natural killer cell-mediated inhibition of HIV-1  
705 replication based on distinct KIR/HLA subtypes. *J Exp Med* **204**:3027-3036.
- 706 47. **Martin MP, Gao X, Lee JH, Nelson GW, Detels R, Goedert JJ, Buchbinder S,**  
707 **Hoots K, Vlahov D, Trowsdale J, Wilson M, O'Brien SJ, Carrington M.** 2002.  
708 Epistatic interaction between KIR3DS1 and HLA-B delays the progression to  
709 AIDS. *Nat Genet* **31**:429-434.
- 710 48. **Chang JJ, Altfeld M.** 2010. Innate immune activation in primary HIV-1 infection.  
711 *J Infect Dis* **202 Suppl 2**:S297-301.
- 712 49. **Cohen GB, Gandhi RT, Davis DM, Mandelboim O, Chen BK, Strominger JL,**  
713 **Baltimore D.** 1999. The selective downregulation of class I major

- 714 histocompatibility complex proteins by HIV-1 protects HIV-infected cells from NK  
715 cells. *Immunity* **10**:661-671.
- 716 50. **Chan CJ, Smyth MJ, Martinet L.** 2014. Molecular mechanisms of natural killer  
717 cell activation in response to cellular stress. *Cell Death Differ* **21**:5-14.
- 718 51. **Norman JM, Mashiba M, McNamara LA, Onafuwa-Nuga A, Chiari-Fort E,**  
719 **Shen W, Collins KL.** 2011. The antiviral factor APOBEC3G enhances the  
720 recognition of HIV-infected primary T cells by natural killer cells. *Nat Immunol*  
721 **12**:975-983.
- 722 52. **d'Ettorre G, Andreotti M, Carnevalini M, Andreoni C, Zaffiri L, Vullo V, Vella**  
723 **S, Mastroianni CM.** 2006. Interleukin-15 enhances the secretion of IFN-gamma  
724 and CC chemokines by natural killer cells from HIV viremic and aviremic patients.  
725 *Immunol Lett* **103**:192-195.
- 726 53. **Mueller YM, Katsikis PD.** 2010. IL-15 in HIV infection: pathogenic or therapeutic  
727 potential? *Eur Cytokine Netw* **21**:219-221.
- 728 54. **Mueller YM, Bojczuk PM, Halstead ES, Kim AH, Witek J, Altman JD, Katsikis**  
729 **PD.** 2003. IL-15 enhances survival and function of HIV-specific CD8+ T cells.  
730 *Blood* **101**:1024-1029.
- 731 55. **Amicosante M, Poccia F, Gioia C, Montesano C, Topino S, Martini F,**  
732 **Narciso P, Pucillo LP, D'Offizi G.** 2003. Levels of interleukin-15 in plasma may  
733 predict a favorable outcome of structured treatment interruption in patients with  
734 chronic human immunodeficiency virus infection. *J Infect Dis* **188**:661-665.
- 735 56. **Walter J, Ghosh MK, Kuhn L, Semrau K, Sinkala M, Kankasa C, Thea DM,**  
736 **Aldrovandi GM.** 2009. High concentrations of interleukin 15 in breast milk are

- 737 associated with protection against postnatal HIV transmission. *J Infect Dis*  
738 **200**:1498-1502.
- 739 57. **Eberly MD, Kader M, Hassan W, Rogers KA, Zhou J, Mueller YM, Mattapallil**  
740 **MJ, Piatak M, Jr., Lifson JD, Katsikis PD, Roederer M, Villinger F, Mattapallil**  
741 **JJ.** 2009. Increased IL-15 production is associated with higher susceptibility of  
742 memory CD4 T cells to simian immunodeficiency virus during acute infection. *J*  
743 *Immunol* **182**:1439-1448.
- 744 58. **Mueller YM, Do DH, Altork SR, Artlett CM, Gracely EJ, Katsetos CD, Legido**  
745 **A, Villinger F, Altman JD, Brown CR, Lewis MG, Katsikis PD.** 2008. IL-15  
746 treatment during acute simian immunodeficiency virus (SIV) infection increases  
747 viral set point and accelerates disease progression despite the induction of  
748 stronger SIV-specific CD8+ T cell responses. *J Immunol* **180**:350-360.
- 749 59. **Steel JC, Waldmann TA, Morris JC.** 2012. Interleukin-15 biology and its  
750 therapeutic implications in cancer. *Trends Pharmacol Sci* **33**:35-41.
- 751 60. **Epardaud M, Elpek KG, Rubinstein MP, Yonekura AR, Bellemare-Pelletier A,**  
752 **Bronson R, Hamerman JA, Goldrath AW, Turley SJ.** 2008. Interleukin-  
753 15/interleukin-15R alpha complexes promote destruction of established tumors  
754 by reviving tumor-resident CD8+ T cells. *Cancer Res* **68**:2972-2983.
- 755 61. **Barouch DH, Whitney JB, Moldt B, Klein F, Oliveira TY, Liu J, Stephenson**  
756 **KE, Chang HW, Shekhar K, Gupta S, Nkolola JP, Seaman MS, Smith KM,**  
757 **Borducchi EN, Cabral C, Smith JY, Blackmore S, Sanisetty S, Perry JR,**  
758 **Beck M, Lewis MG, Rinaldi W, Chakraborty AK, Pognard P, Nussenzweig**

- 759 **MC, Burton DR.** 2013. Therapeutic efficacy of potent neutralizing HIV-1-specific  
760 monoclonal antibodies in SHIV-infected rhesus monkeys. *Nature* **503**:224-228.
- 761 62. **Halper-Stromberg A, Lu CL, Klein F, Horwitz JA, Bournazos S, Nogueira L,**  
762 **Eisenreich TR, Liu C, Gazumyan A, Schaefer U, Furze RC, Seaman MS,**  
763 **Prinjha R, Tarakhovsky A, Ravetch JV, Nussenzweig MC.** 2014. Broadly  
764 neutralizing antibodies and viral inducers decrease rebound from HIV-1 latent  
765 reservoirs in humanized mice. *Cell* **158**:989-999.
- 766  
767  
768

769 **Figure Legends**

770

771 **Figure 1. The IL-15 superagonist treatment of human PBMCs increases their**  
772 **cytotoxic activity. (A)** Schematic structure of the IL-15 superagonist. **(B)** Intracellular  
773 perforin expression and **(C)** intracellular granzyme B expression in CD3<sup>-</sup>CD16<sup>+</sup>CD56<sup>+</sup>  
774 cells were determined by flow cytometry after human PBMCs from six seronegative  
775 donors were incubated for 2 days with the indicated concentration of the IL-15  
776 superagonist and the data represents the mean +/- SEM of MFI values obtained from  
777 the six donors. **(D)** After human PBMCs were stimulated with the indicated  
778 concentration of the IL-15 superagonist for 16 hours, they were co-incubated with K562  
779 target cells (5:1 E:T ratio) for 4 hours and CD107a expression by CD3<sup>-</sup>CD56<sup>+</sup>NK cells  
780 was determined by flow cytometry. The results are expressed as the mean ± STE  
781 percentage of CD107a positive CD3<sup>-</sup>CD56<sup>+</sup> NK cells from PBMCs isolated from 4  
782 normal donors. **(E)** Human PBMCs were cultured with K562 cells at the indicated E:T  
783 ratio with or without the IL-15 superagonist (10 nM). After 3 days, the fraction of dead  
784 K562 cells was quantified by flow cytometry. **(F)** Human PBMCs were cultured with  
785 activated ACH2 cells with or without the indicated dose of the IL-15 superagonist. After  
786 24 hours, the percent cell lysis of target cells was measured using the CytoTox-One  
787 Homogeneous Membrane Integrity Assay. Data represents at least three replicates per  
788 group with mean ± SEM of the group. \*  $P < 0.05$ , \*\*  $P \leq 0.01$ , \*\*\* $P \leq 0.001$ , Student's  $t$   
789 test.

790 **Figure 2. Treatment of hu-spl-PBMC-NSG mice with the IL-15 superagonist**  
791 **inhibited acute *in vivo* HIV-1 infection.** NSG mice were intrasplenically injected with

792 activated human PBMCs ( $\sim 8 \times 10^6$  cells) and with HIV-LucR ( $1 \times 10^7$  IU) and one day  
793 later were either untreated or intravenously treated with the IL-15 superagonist (0.2  
794 mg/kg). **(A)** Five days after HIV-LucR inoculation, the level of HIV-1 infection in the  
795 treated mice was evaluated by measuring LucR activity in splenic lysates. **(B)** Four days  
796 after HIV-LucR inoculation, *in vivo* infection in the mice was evaluated by intravenously  
797 injecting them with a luciferase bioluminescent substrate and then scanning the mice  
798 with the IVIS Spectrum imager to measure the bioluminescence intensity in the spleens.  
799 Pseudocolor images of the bioluminescent intensity measured as photon counts/second  
800 overlaid with gray-scale images of a control uninoculated mouse and IL-15 superagonist  
801 or PBS-treated mice are shown. **(C)** Quantification of the total flux of the bioluminescent  
802 signals detected by the IVIS Spectrum imager reported as photons/second in IL-15  
803 superagonist or PBS-treated mouse spleens. \*\*  $P \leq 0.01$ , Student's *t* test. The  
804 experimental protocol is shown at the bottom of the Figure.

805 **Figure 3. Effect of *in vivo* IL-15 superagonist treatment and/or HIV-1 infection on**  
806 **the population of human NK cells and T cells in hu-spl-PBMC-NSG mouse**  
807 **spleens.** NSG mice were intrasplenically injected with activated human PBMCs ( $\sim 8 \times$   
808  $10^6$  cells). In parallel, some of these mice were also inoculated by intrasplenic injection  
809 of HIV-LucR ( $1 \times 10^7$  IU). One day later, some of the uninoculated and HIV-LucR-  
810 inoculated mice were intravenously treated with the IL-15 superagonist (0.2 mg/kg). Six  
811 days later, the spleens were harvested and after gating on the live human CD45<sup>+</sup>  
812 population, the fraction of splenocytes that were **(A)** NK cells (CD3<sup>-</sup>CD56<sup>+</sup>CD16<sup>+</sup>) or T  
813 cells (CD3<sup>+</sup>) and **(B)** CD8<sup>+</sup> T cells or CD4<sup>+</sup> T cells was determined by flow cytometry.

814 The mean value  $\pm$  SEM of each group of hu-spl-PBMC-NSG mice which were HIV-  
815 LucR-inoculated and/or IL-15 superagonist-treated as indicated is shown.

816 **Figure 4. IL-15 superagonist-treatment of hu-spl-PBMC-NSG mice administered**

817 **three days after inoculation inhibited acute *in vivo* HIV-1 infection.** Three days

818 after NSG mice were intrasplenically injected with activated human PBMCs ( $\sim 8 \times 10^6$

819 cells) and HIV-LucR ( $1 \times 10^7$  IU), the mice were either untreated or treated with one

820 intravenous dose of the IL-15 superagonist (0.2 mg/kg). **(A)** Five days after HIV-LucR

821 inoculation, the level of HIV-1 infection in the IL-15 superagonist-treated mice and

822 untreated mice were evaluated by measuring LucR activity in splenic lysates. **(B)** HIV-1

823 infection was quantified by measuring LucR activity in the splenic lysates in another

824 experimental group at 14 days after inoculation and in another experimental group 21

825 days after inoculation after HIV-LucR inoculation. A dot plot showing the LucR value

826 from each mouse is shown with mean  $\pm$  SEM of the group. \*  $P < 0.05$ , Student's  $t$  test.

827 The experimental protocol is shown at the bottom of the Figure.

828 **Figure 5. NK cells mediate IL-15 superagonist-inhibition of HIV-1 infection in hu-**

829 **spl-PBMC-NSG mice.** Activated PBMCs that were unfractionated or were depleted of

830  $CD8^+$  T cells or NK cells by immunomagnetic sorting were intrasplenically injected into

831 NSG mice ( $\sim 8 \times 10^6$  cells) in parallel with HIV-LucR ( $1 \times 10^7$  IU). One day later, the

832 mice were treated with an intravenous dose of the IL-15 superagonist or PBS. **(A)** The

833 effectiveness of the depletion of  $CD8^+$  T cells or  $CD56^+$  NK cells from the PBMCs prior

834 to injection was assessed by flow cytometry after staining with antibodies to human

835 CD3, CD8 and CD56. **(B)** Six days after intrasplenic injection, HIV-1 infection in the

836 spleens of the mice treated as indicated was quantified by measuring LucR activity in

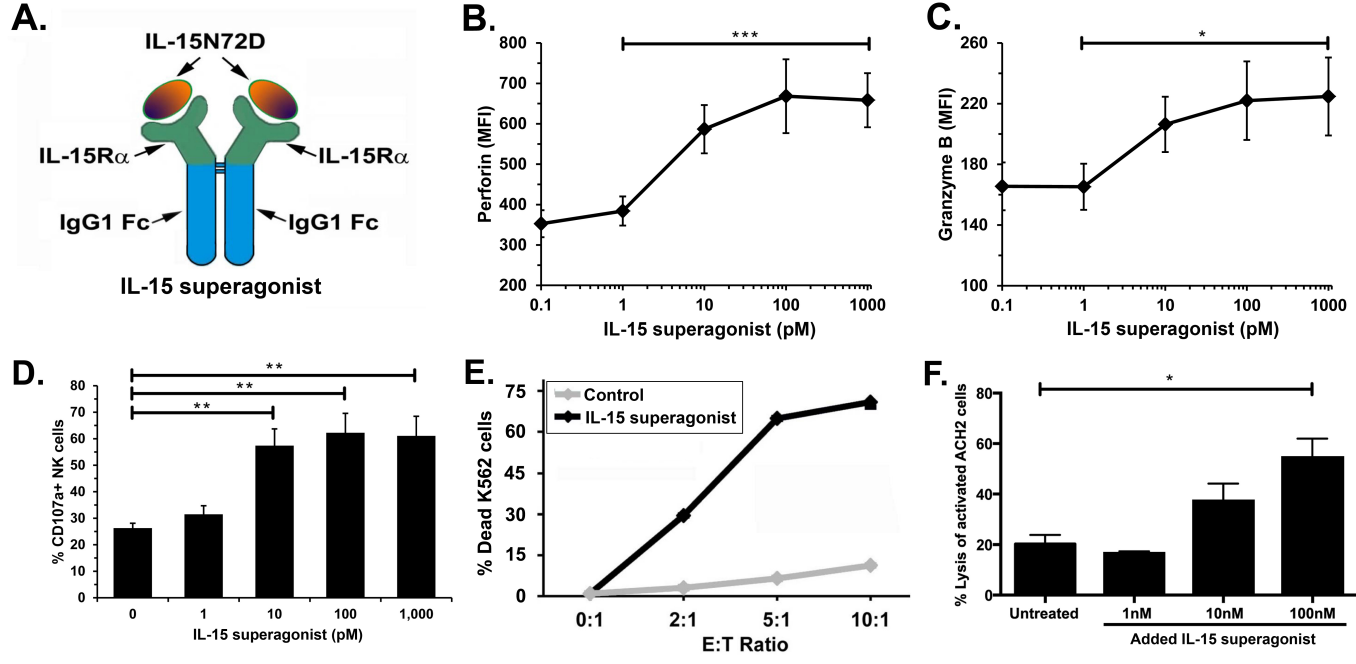
837 the splenic lysates. A dot plot showing the LucR value from each mouse is shown with  
838 mean  $\pm$  SEM of the group. \*\*\*\*  $P < 0.0001$ , Student's  $t$  test

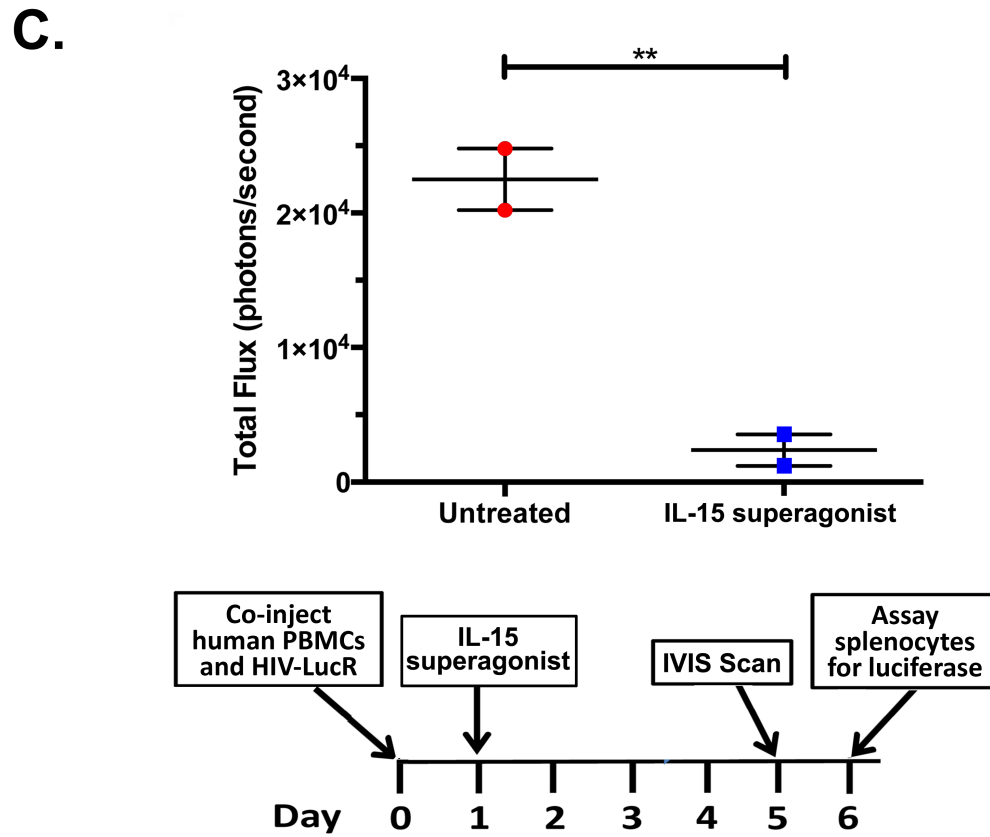
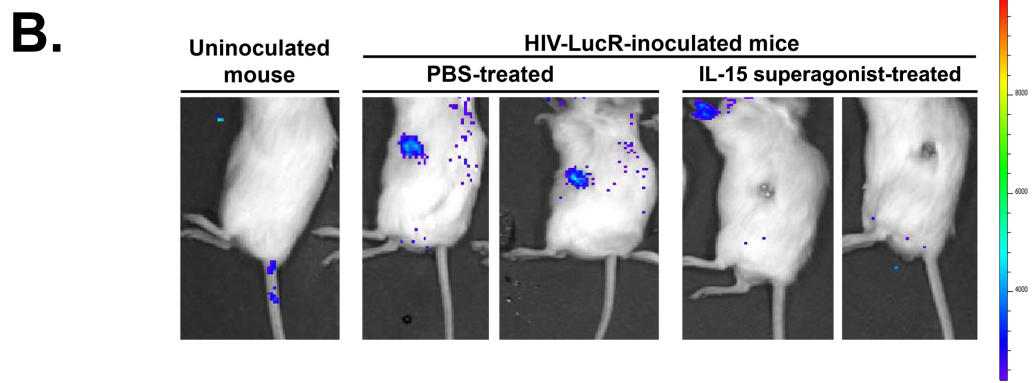
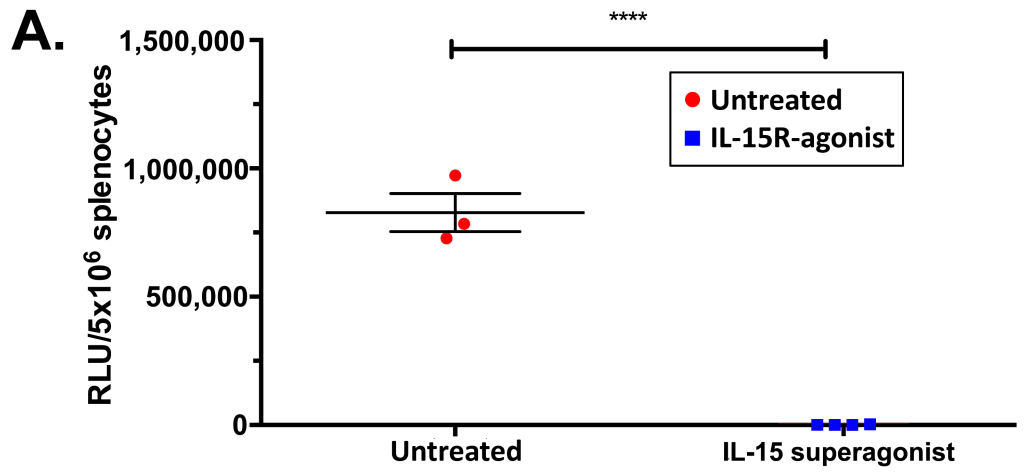
839 **Figure 6. *In vivo* activation of human NK cells by the IL-15 superagonist in the**  
840 **spleens of HIV-1-infected hu-spl-PBMC-NSG mice.** NSG mice were intrasplenically  
841 injected with human PBMCs ( $\sim 8 \times 10^6$  cells) and in parallel inoculated with HIV-LucR ( $1$   
842  $\times 10^7$  IU) and then either untreated or treated with one intravenous dose of the IL-15  
843 superagonist (0.2 mg/kg) one day after infection. Two days later, the harvested  
844 splenocytes were analyzed by flow cytometry for expression of human CD3, CD56,  
845 CD16 and CD69. After gating on the human CD3<sup>+</sup>/CD56<sup>+</sup>/CD16<sup>+</sup> NK cell population, the  
846 fraction of NK cells expressing CD69 was determined. The data point for each mouse is  
847 shown with mean  $\pm$  SEM of the group. \*\*\*  $P < 0.001$ , Student's  $t$  test. The experimental  
848 protocol is shown at the bottom of the Figure.

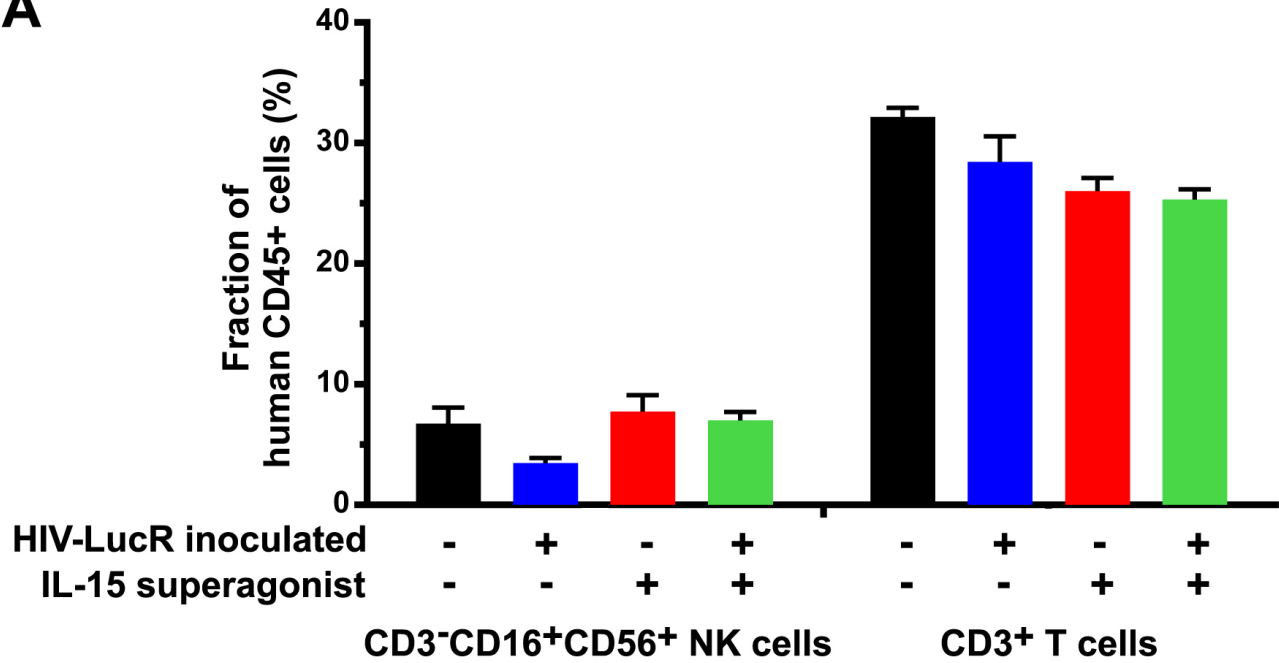
849 **Figure 7. *In vivo* activation of human NK cells by the IL-15 superagonist**  
850 **stimulates elimination of HIV-1-infected cells in the spleens of HIV-1-infected hu-**  
851 **spl-PBMC-NSG mice.** Five days after NSG mice were intrasplenically injected with  
852 human PBMCs ( $\sim 8 \times 10^6$  cells) and in parallel inoculated with HIV-LucR ( $1 \times 10^7$  IU),  
853 they were either untreated or treated with one intravenous dose of the IL-15  
854 superagonist (0.2 mg/kg). One day later, HIV-1 infection in the mouse spleens was  
855 quantified by measuring LucR activity in the splenic lysates. A dot plot showing the  
856 LucR value from each mouse is shown with mean  $\pm$  SEM of the group. \*\*  $P < 0.01$ ,  
857 Student's  $t$  test. The experimental protocol is shown at the bottom of the Figure.

858

859





**A****B**